The thickness of the HI gas layer in spiral galaxies

Sicking, Floris Jan

5 The Mass Distributions in NGC 3198 and NGC 2403

5.1 Introduction

The radial mass distributions in NGC 3198 and NGC 2403 have already been determined before, from observed HI rotation velocities (Begeman 1989, A&A, and Begeman 1987, Ph.D. thesis, Chapter 5). The vertical mass distributions in the two galaxies, however, have hardly any influence on the observed HI rotation velocities, and so they must be determined otherwise.

For this purpose it is assumed that the gas layer of each of the two galaxies is in hydrostatic equilibrium in the vertical direction. Basically this means that in the vertical direction the layer is not contracting or expanding, and that the thickness of the layer is completely determined by the vertical random velocity dispersion of the gas and the vertical mass distribution of the galaxy. Because the gas is collisionly dominated matter, it can safely be assumed that its observed random velocity dispersion, which is along the line of sight, is equal to its vertical random velocity dispersion.

On the basis of this principle, in this chapter the flattening of the mass distributions in NGC 3198 and NGC 2403 will be derived from the HI random velocity dispersions and layer thicknesses measured in Chapter 4.

5.2 Mass Models

Usually the mass distribution in a spiral galaxy is separated in three components:

The first mass component corresponds to the distribution of the light in the galaxy. Usually it is divided in a disk and a bulge. If the mass to light ratios of the disk and bulge are independent of radius, the mass surface densities of the disk and bulge can be traced with the observed radial luminosity profile of the galaxy. In NGC 2403 and NGC 3198 this profile is well represented by an exponential disk, and no bulge (Kent 1987, and Begeman 1987, Ph.D. thesis). So, here the bulge need not be considered.

The density of the disk is denoted as $\rho_{\rm D}$, its scale length as $R_{\rm 0D}$, and its central density as $\rho_{\rm 0D}$. In the vertical direction the disk is assumed to have a sech^2 profile with a scale height, denoted as $Z_{\rm 0D}$, that is not dependent on radius, and equal to $0.2R_{\rm 0D}$ (van der Kruit and Searle 1981). So the density distribution of the disk is given by:

$$\rho_{\rm D}(R,Z) = \rho_{\rm 0D}\exp(-R/R_{\rm 0D})\,{\rm sech}^2(Z/Z_{\rm 0D})\,. \tag{5.1}$$

The total mass of the disk, $M_{\rm D}$, is found by integrating this density distribution in R and Z, which yields:

$$M_{\rm D} = 4\pi R_{\rm 0D}^2 Z_{\rm 0D}\rho_{\rm 0D}\,. \tag{5.2}$$

The second mass component is needed to explain the high observed HI rotation velocities in the outerparts of spiral galaxies (e.g. van Albada et al. 1985). It has no visible counterpart, and it is usually referred to as a dark halo. A suitable density distribution for the dark halo, denoted as $\rho_{\rm H}$, is given by:

$$\rho_{\rm H}(R,Z) = \rho_{\rm 0H}\left(1+\frac{R^2+Z^2/q^2}{R_{\rm H}^2}\right)^{-1}\,. \tag{5.3}$$

This density distribution is a function of three parameters: a core radius, $R_{\rm H}$, a central density, $\rho_{\rm 0H}$, and the ratio between its vertical and radial extent, q. At infinitely large radii it causes an asymptotic rotation velocity, $v_{\rm H}(\infty)$, and in the principal plane of the density distribution, given by $Z=0$, this rotation velocity is given by:

$$v_{\rm H}^2(\infty) = 4\pi G\,\rho_{\rm 0H}\,R_{\rm H}^2\,q\,\arcsin(e)/e\,. \tag{5.4}$$

with $e = \sqrt{1-q^2}$ (Sackett and Sparke 1990). The asymptotic rotation velocity can in several cases directly be compared to the observed HI rotation velocities in the outer parts of spiral galaxies.

The third mass component is the gas. It primarily consists of HI, helium, and possibly molecular hydrogen. The distribution of the HI is observed.

The distribution of the helium cannot be observed, but it is assumed to be the same as that of the HI, and the helium mass is taken into account by multiplying the HI density by a factor of 1.4. The molecular hydrogen is not taken into account (see also Begeman 1987, Ph.D. thesis, page 116), but it is assumed to follow the distribution of the light, and therefore to be included in the first mass component.

When the disk–halo–gas mass model is fitted to observations, the scale length of the stellar disk and the density distribution of the gas are directly inferred from optical and HI line observations. (The scale height of the disk is assumed to be coupled to its scale length.) This leaves the mass of the stellar disk, and the core radius, asymptotic rotation velocity, and flattening of the dark halo as parameters still to be determined from the observed HI rotation velocities, random velocity dispersions, and layer thickness.

First consider how the observed HI rotation velocities can be used for this purpose. The rotation velocities from the different components of the mass model depend on the same parameters as the density distributions of these components (see Appendix A), and add quadratically. So, to obtain the remaining parameters of the disk and the halo, the rotation velocities induced by the model can be fitted to observed rotation velocities. However, usually the observed HI rotation velocities can be explained about equally well with several sets of disk–halo parameters. It appears that a combination of a heavy stellar disk and a dark halo with a large core radius is just as acceptable as a combination of a light stellar disk and a halo with a small core radius, and also that all halo flattenings are acceptable.

Therefore, in order to choose between these different sets of acceptable disk–halo parameters, the observed HI random velocity dispersions and layer thicknesses will be used. For this purpose, the model layer thicknesses are calculated from the observed random velocity dispersions, for the different sets of disk–halo parameters, and compared to the actually observed layer thicknesses. Since the density of the disk falls off exponentially with radius and the density of the dark halo only with the square of the radius, at small radii the stellar disk yields the most important contribution to the mass density in the plane of the galaxy, and at large radii the dark halo. Therefore, at small radii the mass of the stellar disk can be derived; since the disk is relatively thin, a heavy stellar disk will lead to a small layer thickness, and vice versa. At large radii the halo flattening can be derived: the rounder the halo the larger the layer thickness.

5.3 The Theoretical Vertical Density Profile of the Gas

As mentioned in the introduction, to calculate the theoretical gas layer thickness in the mass models described in the previous section, the gas layer is assumed to be in hydrostatic equilibrium in the vertical direction. For a thin layer this means that the dependence of the gas density on the vertical coordinate is given by:

$$\frac{\partial \rho_{\mathrm{gas}}}{\partial Z} = K_Z \frac{\rho_{\mathrm{gas}}}{\sigma^2_{\mathrm{gas}}} \,. \tag{5.5}$$

In this equation ρ_{gas} indicates the density of the gas, σ_{gas} the random velocity dispersion of the gas, which is assumed constant with height above the plane of the layer, and K_Z the total vertical force on the gas per unit of its mass. K_Z is the sum of the forces from the disk, the halo, and the gas itself:

$$K_Z = K_{Z\mathrm{D}} + K_{Z\mathrm{H}} + K_{Z\mathrm{gas}} \,. \tag{5.6}$$

The gravitational forces from the disk and halo can be calculated directly (see Appendix A), and the gravitational force from the gas itself with the Poisson equation in a cylindrically symmetric system (Binney and Tremaine 1987, page 48):

$$-\frac{\partial K_{Z\mathrm{gas}}}{\partial Z} = 4\pi G\, \rho_{\mathrm{gas}} + \frac{1}{R}\frac{\partial R\, K_{R\mathrm{gas}}}{\partial R} = 4\pi G\, \rho_{\mathrm{gas}} - \frac{1}{R}\frac{\partial v^2_{\mathrm{gas}}}{\partial R} \,, \tag{5.7}$$

with the boundary condition that in the plane of the layer it is zero:

$$K_{Z\mathrm{gas}}(Z{=}0) = 0 \,. \tag{5.8}$$

In equation (5.7) $K_{R\mathrm{gas}}$ indicates the gravitational force of the gas in the radial direction, and v_{gas} the rotation velocity induced by the gas. Both are calculated from the spatial distribution of the gas (see Appendix A).

As boundary condition for equation (5.5) we use the constraint that the integral of the density of the gas in the vertical direction yields the surface density of the gas:

$$\int_{-\infty}^{+\infty} dZ \rho_{\mathrm{gas}} = \Sigma_{\mathrm{gas}} \,. \tag{5.9}$$

The layer thickness is defined as the dispersion of the density distribution of the gas in the vertical direction:

$$Z^2_{0\mathrm{gas}} = \frac{1}{\Sigma_{\mathrm{gas}}} \int_{-\infty}^{+\infty} dZ Z^2 \rho_{\mathrm{gas}} \,, \tag{5.10}$$

and it can be obtained after equation (5.5) has been integrated in Z.

5.4 NGC 3198

The Radial Mass Distribution

In NGC 3198 the radial luminosity profile is well explained with an exponential disk with a scale length of 2.6 kpc only (Begeman 1987, Ph. D. thesis, Chapter 2), and no bulge. The scale height of the disk is assumed to be 0.2 times the scale length (van der Kruit and Searle 1981), or 0.52 kpc.

$M_{\rm D}$ $10^{10} M_\odot$	$R_{\rm H}$ kpc	$v_{\rm H}(\infty)$ km/s	q	χ^2
3.570	11.1	177.1	1.0	2.35
3.582	12.0	174.1	0.5	2.38
3.587	12.8	172.0	0.2	2.41
3.589	13.1	171.2	0.1	2.41
1.785	2.00	141.9	1.0	4.19
1.791	2.26	141.3	0.5	4.28
1.794	2.48	140.8	0.2	4.34
1.794	2.58	140.7	0.1	4.36
.7142	.688	145.4	1.0	5.34
.7163	.805	145.3	0.5	5.27
.7174	.906	145.2	0.2	5.22
.7178	.948	145.2	0.1	5.20

Table 5.1 **Parameters of disk–halo mass models fitted to the observed HI rotation velocities in NGC 3198.** In the upper panel the results are presented obtained with the disk mass, halo core radius, and the asymptotic halo rotation velocity as free parameters. In this way the maximum disk mass, $M_{\rm Dmax}$, of $\sim 3.6 \cdot 10^{10} M_\odot$ is obtained, for which the rotation velocities predicted by the disk–halo model do just not exceed the observed HI rotation velocities. In the lower two panels the results are presented obtained with only the halo core radius and halo asymptotic rotation velocity as free parameters, and the disk mass kept fixed at 0.5 and 0.2 times its maximum value. In all fits the axis ratio of the halo has been kept fixed.

To constrain the remaining parameters in the disk–halo–gas mass model for NGC 3198, the model rotation velocities are fitted to the observed HI rotation velocities (see table 5.1). In the fit the rotation velocities induced by the gas are taken into account. They are calculated from the surface densities of the HI (see Appendix A), multiplied by a factor of 1.4 to take the mass of the helium into account. For simplicity, the vertical extent of the gas layer is neglected in the calculation (see also Begeman 1987, Ph.D. thesis page 116–117). The errors introduced in this way will not be large, in the first place because the influence of the vertical extent of gas layer on the induced rotation velocities is not large, and in the second place because the rotation velocities induced by the gas are small compared to the rotation velocities induced by the disk and the halo, and are therefore not an important factor anyway.

In the fitting of the disk–halo models to the observed HI rotation velocities, initially a range of values for the halo flattening and the disk mass is

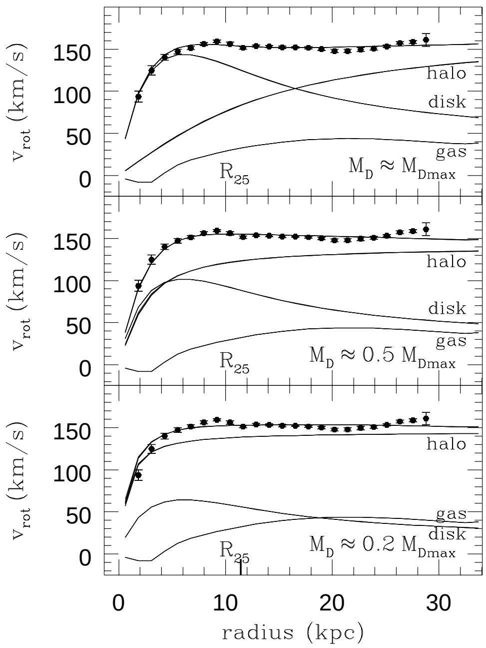

Figure 5.1 **The rotation velocities in the disk–halo models for NGC 3198.** The observed rotation velocities are indicated by the dots with the error bars, indicating 1σ-uncertainties, and the rotation velocities of the model and its three components by the thin solid lines. The three panels correspond to the panels in Table 5.1. In each panel the results for fixed halo axis ratios of 1.0, 0.5, 0.2, and 0.1 are shown, but these cannot be distinguished.

adopted. The precise values are to be determined later, from the observed HI random velocity dispersions and layer thicknesses. First however, the maximum disk mass, which is the disk mass corresponding to the maximum disk–halo rotation velocities allowed by the observed HI rotation velocities, is determined. After the maximum disk mass has been obtained, the fitting is done with only the halo core radius and asymptotic rotation velocity as free parameters, while the disk mass is kept fixed at 0.5 and 0.2 times the obtained maximum disk mass. All this is done for various halo flattenings.

With all disk masses and halo flattenings the observed HI rotation velocities are represented equally well (see figure 5.1). The maximum disk mass found here is somewhat higher ($\sim$10%) than the maximum disk mass for a round halo found by Begeman (1987, thesis, page 127). This may be because Begeman derived the radial mass distribution of the stellar disk directly from the observed radial luminosity profile of the galaxy, and did not use a fitted exponential disk. So, while Begeman's disk is truncated where the photometry stops, the exponential disk used in this study will extend to infinite radii, and therefore it will also have a higher mass.

The Flattening of the Mass Distribution

To find the disk mass and the flattening of the dark halo for the models fitted in the previous section (see table 5.1), the thickness of the HI layer is calculated from the observed random HI velocity dispersions smoothed as a function of radius (see figure 4.7) and the overall force field, taking into account the self-gravity of the gas. We then compare the calculated values to the observed HI layer thickness.

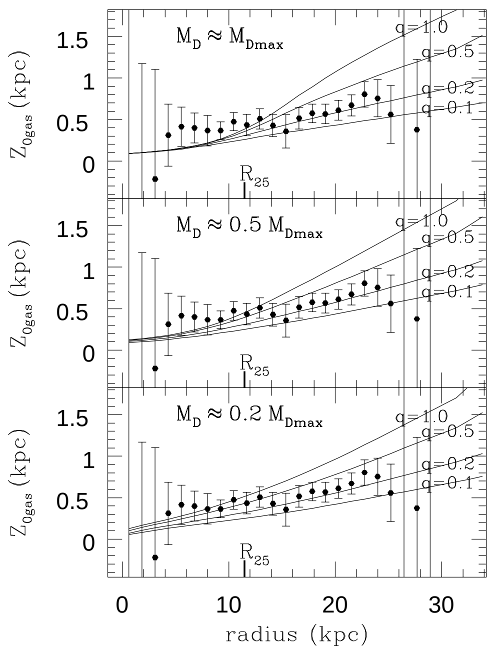

Figure 5.2 **The gas layer thickness in the disk–halo models for NGC 3198.** The thin solid lines indicate the theoretical, and the dots with the error bars (indicating 1σ-uncertainties) the observed layer thickness. The three panels correspond to the panels in Table 5.1. In each panel the model layer thickness is given for halo axis ratios of 1.0, 0.5, 0.2, and 0.1.

From Figure 5.2 we can see that for all disk masses, a halo axis ratio of about 0.2 is in agreement with the observed HI layer thicknesses at large radius. A dark halo rounder than say $q = 0.4$ seems unlikely. At small radii the model layer thickness is too low, although within the uncertainties of the observed layer thicknesses. A disk mass lower than the maximum disk mass may be preferable, since with a light stellar disk higher values for the layer thickness are predicted.

However, the determination of the actual disk mass and halo core radius from the measured HI random velocity dispersion and layer thickness works less well than would be expected. The reason is that mass models with a heavy stellar disk and a halo with a large core radius, and mass models with a light stellar disk and a halo with a small core radius, both explaining the observed HI rotation velocities about equally well, also have approximately the same flatness. If the stellar disk is heavy, the mass distribution will be flattened due to the disk itself, and if the stellar disk is light the mass distribution will be flattened due to the small core radius of the dark halo. Therefore these models predict also about the same layer thicknesses.

5.5 NGC 2403

The Radial Mass Distribution

M_D $10^{10} M_\odot$	R_H kpc	$v_H(\infty)$ km/s	q	χ^2
1.683	10.07	177.3	1.0	3.56
1.685	10.70	172.9	0.5	3.56
1.686	11.29	170.1	0.2	3.56
1.687	11.54	169.1	0.1	3.56
1.655	14.13	194.2	0.0	3.02
.8415	1.562	119.3	1.0	4.77
.8424	1.737	118.5	0.5	4.93
.8431	1.884	117.9	0.2	5.04
.8433	1.944	117.7	0.1	5.08
.3366	.8781	125.3	1.0	3.58
.3370	.9894	124.8	0.5	3.64
.3372	1.085	124.5	0.2	3.68
.3373	1.124	124.3	0.1	3.70

Table 5.2 **Parameters of disk-halo mass models fitted to the observed HI rotation velocities in NGC 2403.** In the upper panel the results are presented obtained with the disk mass, halo core radius, and the asymptotic halo rotation velocity as free parameters. In this way the maximum disk mass, M_{Dmax}, of $\sim 1.7 \cdot 10^{10} M_\odot$ is obtained, for which the rotation velocities predicted by the disk–halo model do just not exceed the observed HI rotation velocities. In the lower two panels the results are presented obtained with only the halo core radius and halo asymptotic rotation velocity as free parameters, and the disk mass kept fixed at 0.5 and 0.2 times its maximum value. In all fits the axis ratio of the halo has been kept fixed.

In NGC 2403 the stellar disk has a scale length of 2.05 kpc (Kent 1987), from which a scale height of 0.41 kpc (van der Kruit and Searle 1981) is inferred. The remaining parameters of the disk–halo models fitted to the rotation curve are given in Table 5.2.

At small radii the models do not correctly represent the observed HI rotation velocities (see figure 5.3). Perhaps the observed rotation velocities cannot entirely be trusted, because of the twist in the inner parts of the observed HI velocity field (see figure 4.11, upper right corner). With the addition of a bulge it might also be possible to explain the observed HI rotation velocities, but no stellar bulge is visible in the optical luminosity profile

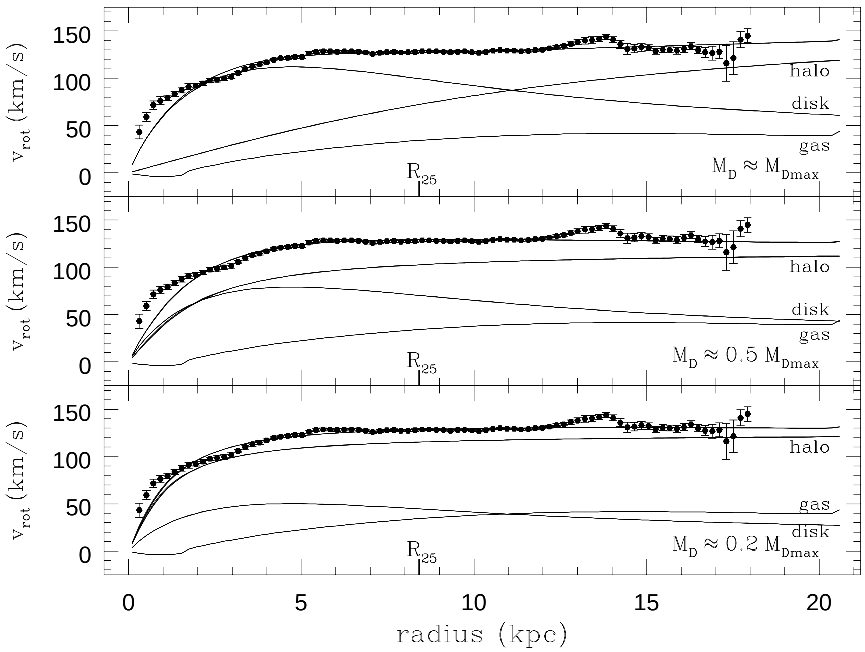

Figure 5.3 **The rotation velocities in the disk-halo models for NGC 2403.** The observed rotation velocities are indicated by the dots with the error bars, indicating 1σ-uncertainties, and the rotation velocities of the model and its three components by the thin solid lines. The three panels correspond to the panels in Table 5.2. In each panel the results for fixed halo axis ratios of 1.0, 0.5, 0.2, and 0.1 are shown, but these cannot be distinguished.

of the galaxy (see Kent 1987). Another explanation may be that the mass-to-light ratio of the visible matter is not constant with radius, but increases at small radii.

The Flattening of the Mass Distribution

On the basis of the comparison between the actually observed layer thickness and the model layer thickness calculated from the observed random velocity dispersions smoothed as a function of radius (see figure 4.15) none of the disk-halo models in Table 5.2 can really be preferred or excluded. However, the effect of a gas layer with a thickness of 0.4–0.5 kpc would have been visible in the observed HI velocity dispersion field as an X-shaped feature, and it is not. Therefore, and also because of the low observed layer thickness at intermediate to large radii, a round halo seems not so likely.

Moreover, in none of the models the layer thickness is constant with radius, as the observed HI layer thicknesses seem to be. For this reason a model with a light disk and flattened halo may be preferable, because in such a model the increase of the layer thickness with radius is weakest. Obviously, beyond about 11 kpc the thickness that is measured is meaningless.

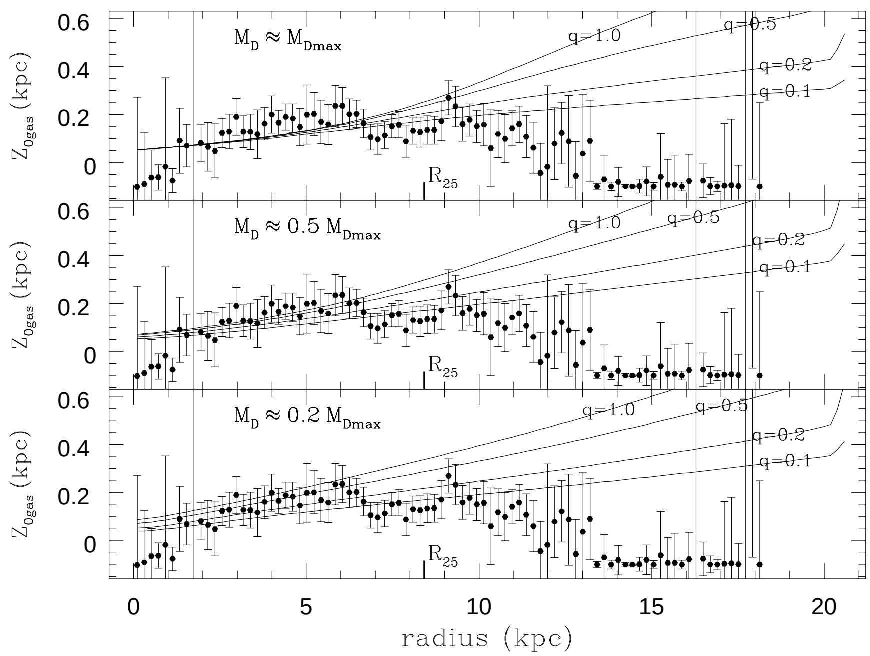

Figure 5.4 **The gas layer thicknesses in the disk–halo models for NGC 2403.** The thin solid lines indicate the theoretical, and the dots with the error bars (indicating 1σ-uncertainties) the observed layer thickness. The three panels correspond to the panels in Table 5.2. In each panel the model layer thickness is given for halo axis ratios of 1.0, 0.5, 0.2, and 0.1.

Appendix A The Rotation Velocities and Vertical Forces Induced by the Various Mass Components

For a disk with a density distribution, $\rho(R,Z)$, the induced rotation velocity, v_{D}, in the plane of the disk, $Z=0$, is calculated with:

$$v_{\mathrm{D}}^2(R) = -8\pi G R \int_0^\infty u du \int_0^\infty dZ \frac{\partial \rho(u,Z)}{\partial u} \frac{\mathcal{K}(p) - \mathcal{E}(p)}{\pi\sqrt{Rup}} \tag{5A.1}$$

with $x = (R^2 + u^2 + Z^2)/(2Ru)$, $p = 1/(x + \sqrt{x^2-1})$, and where $\mathcal{K}$ and $\mathcal{E}$ are the complete elliptic integrals of the first and second kind (Casertano 1983). This expression is evaluated numerically.

For the stellar, exponential–sech^2 disk, described in the text, with its density distribution given by equation (5.1), the vertical gravitational force, $K_{Z\mathrm{D}}$, is equal to:

$$K_{Z\mathrm{D}}(R,Z) = -4\pi G\, \rho_{0\mathrm{D}} \exp(-R/R_{0\mathrm{D}})\ Z_{0\mathrm{D}}\ \tanh(Z/Z_{0\mathrm{D}}) \tag{5A.2}$$

(Spitzer 1942).

For the dark halo, with a density distribution given by equation (5.3), the equation for the gravitational potential has been published by Sackett and Sparke (1990). Differentiation of their equation with respect to R is straightforward and yields the following expression for the rotation velocity of the dark halo, v_{H}, in its principle plane, $Z=0$:

$$v_{\mathrm{H}}^2(R) = v_{\mathrm{H}}^2(\infty) \left(1 - \frac{(e/q)\cdot \arctan\left(\sqrt{(e^2R_{\mathrm{H}}^2 + R^2)\,/\,(q^2R_{\mathrm{H}}^2)}\right)}{\arctan(e/q)\cdot\sqrt{(e^2R_{\mathrm{H}}^2 + R^2)\,/\,(q^2R_{\mathrm{H}}^2)}} \right) \tag{5A.3}$$

with $e = \sqrt{1-q^2}$. For a round halo the rotation velocity is given by equation (5A.3) in the limit $q \rightarrow 1$:

$$v_{\mathrm{H}}^2(R) = v_{\mathrm{H}}^2(\infty) \left(1 - \frac{\arctan(R/R_{\mathrm{H}})}{R/R_{\mathrm{H}}} \right), \tag{5A.4}$$

which has also been given by Begeman (1987, thesis, page 117). For an infinitely flat halo, with an excentricity of one, the rotation velocity is given by equation (5A.3) in the limit $q \rightarrow 0$:

$$v_{\mathrm{H}}^2(R) = v_{\mathrm{H}}^2(\infty) \left(1 - \sqrt{\frac{R_{\mathrm{H}}^2}{R_{\mathrm{H}}^2 + R^2}} \right). \tag{5A.5}$$

The vertical gravitational force of the dark halo, $K_{Z\mathrm{H}}$, is obtained by differentiating Sackett and Sparke's equation for the gravitational potential of the dark halo with respect to Z:

$$K_{Z\mathrm{H}}(R,Z) = -\frac{v_{\mathrm{H}}^2(\infty)}{\arcsin(e)d}(f-g)\,, \tag{5A.6}$$

with: $f=\sqrt{x}\arctan\left(eZ/q\sqrt{x}\right)$, $g=\sqrt{y}\arctan\left(eZ/q\sqrt{y}\right)$, $x=(b+d)/2$, $y=(b-d)/2$, $d=\sqrt{b^2-4ac}$, $a=R_{\mathrm{H}}^2$, $b=R_{\mathrm{H}}^2e^2+R^2+Z^2$, $c=Z^2e^2$, and $e=\sqrt{1-q^2}$. For a round halo, in the limit $q\to 1$, this becomes:

$$K_{Z\mathrm{H}}(R,Z) = -\frac{v_{\mathrm{H}}^2(\infty)R_{\mathrm{H}}Z}{(R^2+Z^2)^{3/2}}\left(\sqrt{\frac{R^2+Z^2}{R_{\mathrm{H}}^2}}-\arctan\sqrt{\frac{R^2+Z^2}{R_{\mathrm{H}}^2}}\right). \tag{5A.7}$$

For a flat halo, in the limit $q\to 0$:

$$K_{Z\mathrm{H}}(R,Z) = -\frac{v_{\mathrm{H}}(\infty)}{d}\left(\sqrt{x}-\sqrt{y}\right) \tag{5A.8}$$

with: $x=(b+d)/2$, $y=(b-d)/2$, $d=\sqrt{b^2-4ac}$, $a=R_{\mathrm{H}}^2$, $b=R_{\mathrm{H}}^2+R^2+Z^2$, and $c=Z^2$.

For the gaseous component, the rotation velocities are calculated with equation (5A.1), just as for the stellar disk. It is assumed that the gas layer is cylindrically symmetric, and for simplicity the vertical extent of the layer is neglected, even though the layer thickness is known. Doing so, the Z dependency of the density becomes a Dirac δ–function. Consequently the integration in Z in equation (5A.1) becomes the evaluation at $Z=0$ of the function that is integrated.

The vertical gravitational force of the gas is found by integrating the Poisson equation (5.7) once. This yields:

$$K_{Z\mathrm{gas}}(R,Z) = -4\pi G\int_0^Z dZ'\,\rho_{\mathrm{gas}} + \frac{Z}{R}\frac{\partial v_{\mathrm{gas}}^2}{\partial R}\,. \tag{5A.10}$$

Appendix B The integration of the equation for hydrostatic equilibrium

To integrate the coupled differential equations (5.5), (5.7), and (5.10) from $Z=0$ to $Z=\infty$ we re-write them as a function of a vector $\vec{u}(Z)$. The first component of this vector is defined as the density of the gas:

$$u_1(Z) = \rho_{\mathbf{gas}}(Z)\,, \tag{5B.1}$$

the second component as the surface density of the gas up to the current Z:

$$u_2(Z) = \int_0^Z dZ' \rho_{\mathbf{gas}}\,, \tag{5B.2}$$

and the third component as the second central moment of the density of the gas up to the current Z:

$$u_3(Z) = \int_0^Z dZ' {Z'}^2 \rho_{\mathbf{gas}}\,. \tag{5B.3}$$

With equation (5A.2) the Z–force of the disk, $K_{Z\mathrm{D}}(Z)$, and with equation (5A.6) the Z–force of the dark halo, $K_{Z\mathrm{H}}(Z)$, can be evaluated, and by substituting equation (5B.2) into (5A.10), the Z–force induced by the gas, $K_{Z\mathbf{gas}}(Z)$ can be written as a function of $\vec{u}$:

$$K_{Z\mathbf{gas}}(Z) = -4\pi G\, u_2(Z) + \frac{Z}{R}\frac{\partial v^2_{\mathbf{gas}}}{\partial R}\,. \tag{5B.4}$$

The total force on the gas, $K_Z(Z)$, is the sum of the forces of the disk, the halo, and the gas itself, and it is evaluated by substituting equation (5B.4) in equation (5.6) of the text. Equations (5.5), (5.9), and (5.10) can then be rewritten as a function of $\vec{u}$:

$$\begin{aligned}
\frac{du_1}{dZ} &= \left(K_{Z\mathrm{D}} + K_{Z\mathrm{H}} - 4\pi G\, u_2 + \frac{Z}{R}\frac{\partial v^2_{\mathbf{gas}}}{\partial R}\right)\frac{u_1}{\sigma^2_{\mathbf{gas}}} \\
\frac{du_2}{dZ} &= u_1 \\
\frac{du_3}{dZ} &= u_1\, Z^2\,.
\end{aligned} \tag{5B.5}$$

To obtain the theoretical vertical density profile of the gas, equation (5B.5) can be integrated in Z, with Bulirsch–Stoer integration, for example (see Numerical Recipes 1992, page 724). The integration is started at $Z=0$ with $u_1(0) = \rho_{\mathbf{gas}}(Z=0)$, $u_2(0) = 0$, and $u_3(0) = 0$. After the integration, at $Z=\infty$, the surface density of the gas is given by:

$$\Sigma_{\mathrm{gas}} = 2u_2(\infty) \tag{5B.6}$$

and the layer thickness by:

$$Z_{0\mathrm{gas}}^2 = u_3(\infty)/u_2(\infty) \tag{5B.7}$$

In practice, usually $\rho_{\mathrm{gas}}(Z=0)$ is not known, however. This means that only part of the boundary condition needed to start the integration is available. Therefore, in practice the observed value for Σ_{gas} is used, as given by equation (5.9). This boundary condition applies to the second element of $\vec{u}$, at $Z=\infty$ instead of $Z=0$, and so it can only be fulfilled after the integration. To solve this problem, subsequent integrations of equation (5B.5) are done in an iterative process. Each integration is started with an estimate $\rho'_{\mathrm{gas}}(Z=0)$ for $\rho_{\mathrm{gas}}(Z=0)$) instead of the actual value. From this estimate, after the integration an estimate Σ'_{gas} is found for Σ_{gas}. In the absence of self-gravitation of the gas, $\rho'_{\mathrm{gas}}(Z=0)/\Sigma'_{\mathrm{gas}}$ will be equal to $\rho_{\mathrm{gas}}(Z=0)/\Sigma_{\mathrm{gas}}$, and in the presence of self-gravitation, at least if the estimate $\rho'_{\mathrm{gas}}(Z=0)$ is not too bad, the two will be close. Therefore, after each integration $\rho'_{\mathrm{gas}}(Z=0)$ is updated with $\rho'_{\mathrm{gas}}(Z=0)\Sigma_{\mathrm{gas}}/\Sigma'_{\mathrm{gas}}$. The process of integrating equation (5B.5), and updating the initial condition is repeated until convergence is reached in Σ_{gas}.

References

van Albada, T.S., Bahcall, J.N., Begeman, K., Sancisi, R.: 1985 *Astrophys.J.* 295, 305

Begeman, K.G.: 1987, Ph.D. thesis, Groningen University

Begeman, K.G.: 1989, *Astron. Astrophys.* 223, 47–60

Begeman, K.G., Broeils, A.H., Sanders, R.H.: 1991, *Mon. Not. R. Astr. Soc.* 249, 523–537

Binney, J., Tremaine, S.: 1987, *Galactic Dynamics*, Princeton University Press

Casertano, S.: 1983 *Mon. Not. R. Ast. Soc.* 203, 735–747

Kent, S.: 1987 *Astrophys. J.* 93, 816

van der Kruit, P.C., Searle, L.: 1981 *Astron. Astrophys.* 95,105

Press, W.H., Teukolsky, S.A., Vetterling, W.T., Flannery, B.P.: 1992, *Numerical Recipes (Second Edition)*, Cambridge University Press

Sackett, P.D., Sparke, L.S.: 1990, *Astrophys. J.* 361, 408–418

Spitzer, L.: 1942, *Astrophys. J.* 95, 329